Theory of sorption hysteresis in nanoporous solids: Part II Molecular condensation

Citation: Bazant, Martin Z., and Zdeněk P. Bažant. "Theory of Sorption Hysteresis in Nanoporous Solids: Part II Molecular Condensation." Journal of the Mechanics and Physics of Solids 60, no. 9 (September 2012): 1660–1675.

As Published: http://dx.doi.org/10.1016/j.jmps.2012.04.015

Publisher: Elsevier

Persistent URL: http://hdl.handle.net/1721.1/99221

Version: Author's final manuscript: final author's manuscript post peer review, without publisher's formatting or copy editing

Theory of Sorption Hysteresis in Nanoporous Solids: II. Molecular Condensation

Martin Z. Bazant[1] and Zdeněk P. Bažant[2]
November 22, 2011

Abstract: Motivated by the puzzle of sorption hysteresis in Portland cement concrete or cement paste, we develop in Part II of this study a general theory of vapor sorption and desorption from nanoporous solids, which attributes hysteresis to hindered molecular condensation with attractive lateral interactions. The classical mean-field theory of van der Waals is applied to predict the dependence of hysteresis on temperature and pore size, using the regular solution model and gradient energy of Cahn and Hilliard. A simple "hierarchical wetting" model for thin nanopores is developed to describe the case of strong wetting by the first monolayer, followed by condensation of nanodroplets and nanobubbles in the bulk. The model predicts a larger hysteresis critical temperature and enhanced hysteresis for molecular condensation across nanopores at high vapor pressure than within monolayers at low vapor pressure. For heterogeneous pores, the theory predicts sorption/desorption sequences similar to those seen in molecular dynamics simulations, where the interfacial energy (or gradient penalty) at nanopore junctions acts as a free energy barrier for snap-through instabilities. The model helps to quantitatively understand recent experimental data for concrete or cement paste wetting and drying cycles and suggests new experiments at different temperatures and humidity sweep rates.

Introduction

As introduced in Part I [1], a long-standing puzzle in the thermodynamics of concrete or cement paste and other nanoporous solids is the pronounced hysteresis of the sorption/desorption isotherm at low vapor pressure [36, 26, 27, 38, 39, 31, 3, 25]. Typical experimental data for wetting/drying cycles in concrete is shown in Fig 1, and similar behavior can be observed (or expected) in many other important situations, such as water sorption in dry soils or wood, carbon sequestration in porous absorbents, and natural gas recovery from nanoporous shales. At low vapor pressures, well below the saturation pressure, very little bulk liquid exists in the larger pores, and so the observed hysteresis cannot be attributed to the classical "ink-bottle effect" of capillarity from continuum fluid mechanics [16, 15]. Moreover, in nanopores, the Laplace tension of a continuous meniscus can easily exceed the tensile strength of the liquid. So it is widely believed that adsorbate layers must be uniformly spread over the entire internal surface area at low vapor pressure and unable to coalesce into nonuniform patches or droplets.

This thinking underlies the ubiquitous method of determining the internal surface area of porous media by fitting the sorption isotherm to the Brunauer-Emmett-Teller (BET) equation of state [17], which is strictly valid only for a statistically homogeneous adsorbate on a flat surface. Since the BET isotherm is perfectly reversible, the internal surface area can only be unambiguously inferred from one type of measurement, either sorption or desorption, starting

---

[1] Associate Professor of Chemical Engineering and Mathematics, Massachusetts Institute of Technology, Cambridge MA 02139.

[2] McCormick Institute Professor and W.P. Murphy Professor of Civil Engineering and Materials Science, Northwestern University, 2145 Sheridan Road, CEE/A135, Evanston, Illinois 60208; z-bazant@northwestern.edu (corresponding author).

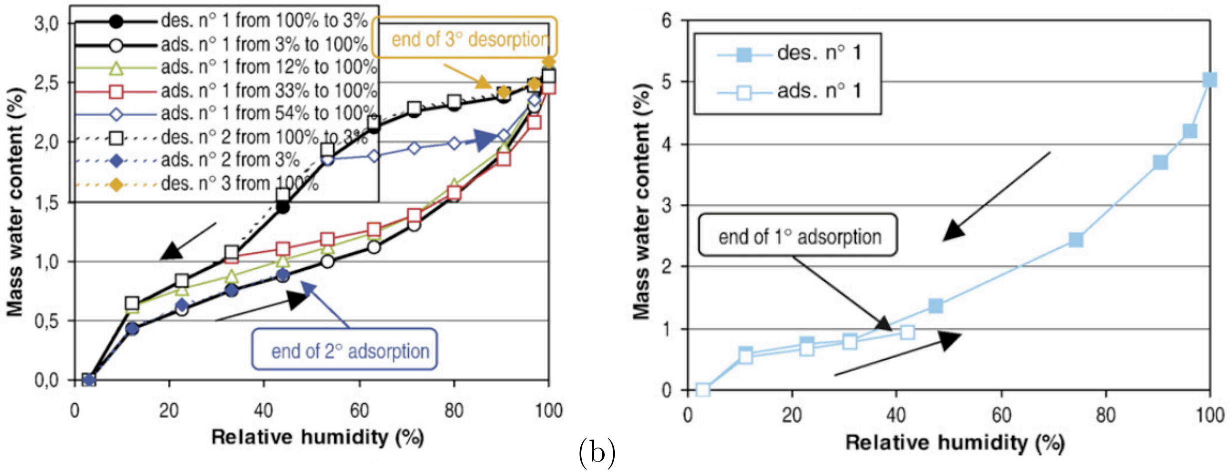

(a) (b)

Figure 1: Experimental data for isothermal water-vapor desorption and sorption cycles in concrete at different temperatures. (a) Pronounced hysteresis at $T = 23°\mathrm{C}$. (b) Suppressed hysteresis at $T = 44°\mathrm{C}$. [Reproduced from Fig. 2(e) and 2(g) of Baroghel-Bouny [44] with permission.]

from a well defined reproducible initial state. Typically, the BET fit is made for sorption starting from very low vapor pressure, assuming that the internal surface is initially bare, but it is troubling to neglect the desorption data, which would imply a different BET internal surface area, without a theory to explain its origin. Moreover, if a mathematical theory could be developed, then in principle one could extract more complete information about the internal pore structure, such as the statistical distributions of pore thickness or pore area, from the history dependence of sorption and desorption.

If one insists on the validity of any reversible adsorption isotherm (not only BET), then the only way to explain the observed hysteresis is to invoke changes in the accessible internal surface area, e.g. due to chemical transformations or structural damage [27, 41, 38, 25, 30]. As a result, this picture of "pore collapse" and subsequent reopening upon desorption and sorption, respectively, is firmly entrenched, but it is noteworthy that, sixty years after the first observations of sorption hysteresis in concrete and cement paste, no mathematical theory has emerged to justify this assumption or make any testable theoretical predictions. For example, it is not clear how the pore collapse hypothesis could explain the strong dependence of sorption hysteresis in concrete on temperature and chemical composition of the vapor observed in recent experiments [44], as shown in Figure 1, or how it could be reconciled with the measured shrinkage values. While some adsorption-related structural changes surely occur in cement paste and concrete and other nanoporous solids, especially at high vapor pressures, the repeatability of sorption hysteresis (after the first few cycles) and the relatively small concomitant macroscopic deformations seem inconsistent with the very drastic changes to the pore structure at the nanoscale required by the pore-collapse hypothesis.

In this work, we show that, due to molecular discreteness, hysteresis is a natural and unavoidable feature of sorption in nanoporous solids with *fixed* pore geometries. In Part I [1], we showed that misfit pressures due to discrete molecular forces around heterogeneities in the nanopore geometry generally provide local energy barriers for the passage of the adsorbate-vapor interface, consistent with evidence from molecular dynamics simulations [19, 20, 22, 23, 21]. As the thermodynamic driving force is increased by changing the vapor pressure, the interface remains pinned at the heterogeneity until a sudden "snap-through instability" occurs, analogous to snap-through buckling of a flat arch. This theory is also reminiscent of the Peierls-Nabarro model of dislocation motion in crystals, where the misfit strain energy due to discrete molecular forces in the dislocation core provides the crucial resistance to dislocation motion, which cannot be predicted by continuum elasticity [54]. A common feature of both theories is the assumption of a layered solid-like material undergoing sudden, localized rearrangements in response to a driving force that overcome the effective "lattice resistance". An important difference between nanopore sorption and dislocation motion, however, is that there is no reference crystal structure or long-range order in the adsorbate, and so much more dramatic molecular rearrangements, such as wetting phase transformations, are possible. Predicting such phase transformations and their dependence on temperature requires a more detailed molecular model.

Here, in Part II, we consider sorption from the general perspective of statistical thermodynamics and develop a simple mathematical theory that connects hysteresis to inter-molecular forces. The model is quantitatively consistent with the concrete sorption data in Figure 1 and suggests new directions for experiments and simulations to further develop the theory. The key insight is that sorption hysteresis is possible at sufficiently low temperature in any fixed surface geometry, as long as the adsorbed molecules have a short-range attraction. Although weaker than the orthogonal forces that bind the adsorbate to the surface, such attractive lateral forces within the adsorbate itself promote condensation into stable high density patches below a critical temperature, regardless of the pore geometry. This phenomenon can be inhibited by geometrical or chemical heterogeneities on the surface, but molecular condensation can also occur in homogeneous pores or on flat surfaces, as the metastable homogeneous adsorbate phase separates into stable low-density and high-density phases within the porous structure.

Before we begin, let us explain our choice of terminology. The term "capillary condensation" has been used to describe wetting/de-wetting transitions on surfaces, which comprise a well-studied class of phase separation phenomena in confined systems [18]. We avoid the use of this term because in many fields, such as cement and concrete research (which motivates our work), the term "capillary water" refers to liquid water at high vapor pressure in large ($> 1\mu$m) pores, which can be modeled by continuum fluid mechanics with constant gas/liquid surface tension. Here, we suggest the term "molecular condensation" to refer to the phase separation of discrete adsorbed molecules in nanopores at low vapor pressure, which requires a statistical mechanical treatment.

Mean-Field Theory of Molecular Condensation

Capillarity at the Molecular Scale: The macroscopic continuum theory of capillarity cannot be applied to very thin adsorbate layers, whose individual molecules interact strongly with the surface – and each other [82, 83, 81, 18]. The density of an adsorbate is generally heterogeneous and lies between that of the bulk liquid and vapor phases, due to attractive forces with the surface which stabilize individual adatoms and (upon contact with a second surface) give rise to disjoining pressure. These "orthogonal forces" allow adsorbed molecules to be distributed over a surface without maintaining close lateral contacts. In a nanoscale pore, the total energy of the missing lateral bonds would be grossly overestimated, if they were approximated by sharp, continuous surfaces using the bulk surface tension and the nanoscale curvature. Instead, one must develop a theory that takes "lateral forces" between discrete adsorbate molecules explicitly into account.

The theory of snap-through instabilities in nonuniform pore geometries from Part I is an

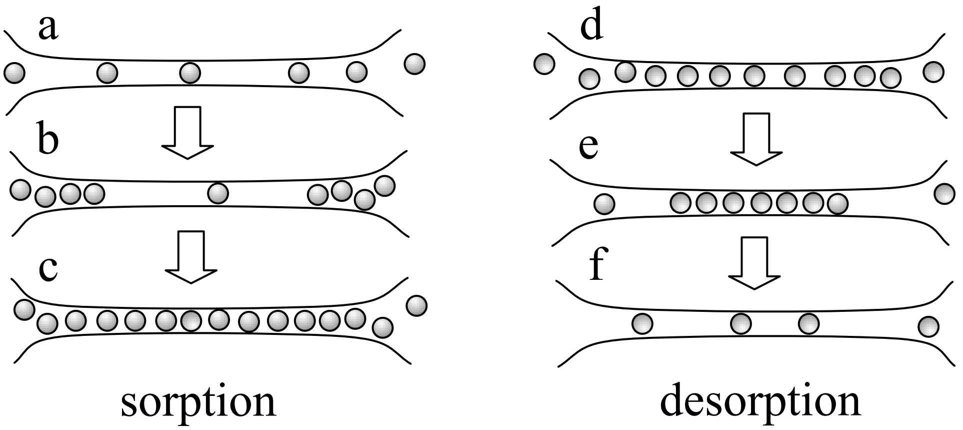

Figure 2: Molecular condensation in a straight, monolayer-thick pore during sorption (left) and desorption (right) from the vapor at low temperature. Attractive lateral forces lead to the spontaneous separation of high-density and low-density adsorbate phases from metastable homogeneous phases. Analogous thermodynamic instabilities of the adsorbate distribution would also occur in thicker pores or flat surfaces, only across a different range of relative humidities, depending on the free energies of adsorption and lateral interaction. In non-uniform pores, the snap-through instability is another manifestation of this general phenomenon, driven by attractive lateral (or inclined) forces in the adsorbate. It naturally leads to sorption hysteresis without invoking any changes in pore structure.

example of such an approach, but the effect of attractive lateral forces is much more general and can lead to sorption hysteresis even in perfectly uniform geometries. The basic idea is already illustrated by the simplest case of monolayer adsorption on a flat bare surface or monolayer-thick pore, as shown in Figure 2. (The latter problem is equivalent to lithium insertion and extraction in a crystalline nanoparticle in a Li-ion battery [68, 69, 67], and we apply similar concepts and models for adsorption dynamics [60].) As humidity increases during sorption (left), the dilute homogeneous adsorbate a becomes thermodynamically unstable and separates b into locally stable low-density and high-density phases, which quickly grow and merge into a stable homogeneous adsorbate at high density c. As humidity then decreases during desorption (right), the homogeneous phase d destabilizes and coalesces to form the stable, dense phase e, which quickly shrinks and leaves behind a stable, homogeneous low-density adsorbate f. The sketches in Figure 2 assume nucleation of the second phase at the pore openings, although other phase-separation pathways are possible.

The key point is that molecular condensation, or separation into low-density and high-density adsorbate phases, is history dependent and occurs by triggering the sudden instability of a metastable state. The specific pore geometry is largely irrelevant. Spontaneous phase separation of the adsorbate is mathematically analogous to the snap-through instability of shells and arches, but the physical interpretation in terms of buckling failure may not always apply. More importantly, in order to predict the effect of temperature on sorption hysteresis, one must go beyond mechanical analogs and consider the statistical thermodynamics of adsorption.

Thermodynamics of Adsorption with Lateral Forces: Consider a nanopore or surface film, whose state is described by a dimensionless filling $\Theta = \Gamma_w/\Gamma_1$, which may depend on lateral position x. The Gibbs free energy per surface site g can be expressed for a homogeneous adsorbate as follows:

$$g_{hom}(\Theta, x) = g_{mix}(\Theta, x) - \Delta g_a(x)\,\Theta \tag{1}$$

where g_{mix} is the free energy of mixing in the pore volume $V_s(x)$ associated with surface site x, which contains an expected number $\Theta(x)$ of adsorbate molecules, whose free energy change (per molecule) due to adsorption from the vapor phase is

$$\Delta g_a = k_B T \ln c_0 + \Delta q_a. \tag{2}$$

The first term is a reference entropy, expressed in terms of a dimensionless concentration c_0 (as in BET theory) and Boltzman's constant k_B, and the second term, Δq_a, is the latent heat of adsorption minus that of liquefaction per site. To focus on molecular effects, here in Part II we define energies per particle, rather than per mole as in Part I ($\frac{\Delta Q_a}{RT} = \frac{\Delta q_a}{k_B T}$), and we drop the overbars for ease of notation. Lateral interactions among adsorbate molecules are included g_{mix}, e.g. according to the regular solution model of the next section. Orthogonal surface-adsorbate forces are treated separately via Δg_a. In the case of pairwise interactions, the enthalpic contribution can be expressed as

$$\Delta q_a = \int_{V_s} d\vec{r} \int_S d\vec{r}_s\ \Phi^s(|\vec{r} - \vec{r}_s)\, p_s(\vec{r}|\vec{r}_s) \tag{3}$$

where the $\Phi^s(r)$ is the pair potential between adsorbate and surface molecules, $p_s(\vec{r}|\vec{r}_s)$ is the conditional probability density of finding a surface molecule at $\vec{r}_s$ anywhere in the solid volume S given an adsorbate molecule at $\vec{r}$ in the pore volume $V_s(x)$ associated with site x. In an isotropic bulk liquid, the pair correlation function $g(r)$ is defined by $p_s(\vec{r}|\vec{r}') = 4\pi r^2 g(r)$ where $r = |\vec{r} - \vec{r}'|$, but here the pore surface breaks symmetry.

Due to attractive lateral interactions, at sufficiently low temperature the homogeneous free energy of mixing $g_{mix}(\Theta)$ becomes non-convex and leads to at least two local minima in the total free energy, corresponding to stable high-density (liquid-like) and low-density (vapor-like) adsorbate phases on the surface, as shown in Fig. 3(a). A common tangent construction connecting the two local minima, which restores convexity across the "miscibility gap", provides the mean free energy of a phase separated system consisting of appropriate proportions of the immiscible endpoint phases (neglecting interphasial tension, discussed below). Phase separation is illustrated by sketches in Figure 2, whose labels correspond to the letters in Figure 3. During sorption, the homogeneous adsorbate passes the low-density free energy minimum a, destabilizes and drops down to the common tangent upon phase separation b, and becomes homogeneous again after passing the high-density free energy minimum c. A similar free-energy path is followed in reverse during desorption, only the free-energy overshoot in the metastable homogeneous adsorbate occurs at high density rather than low density. This is the fundamental source of hysteresis.

The connection with sorption hysteresis becomes more clear from the "diffusional" chemical potential of the homogeneous adsorbate,

$$\mu_{hom} = \frac{dg_{hom}}{d\Theta} = \frac{dg_{mix}}{d\Theta} - \Delta g_a \tag{4}$$

which is the net free energy change to add a molecule (and remove any vacant site). As sketched in Fig. 3(b), a non-convex free energy corresponds to a non-monotonic chemical potential versus composition. In equilibrium, the chemical potential of an adatom equals that of a vapor molecule,

$$\mu_v = k_B T \ln h \tag{5}$$

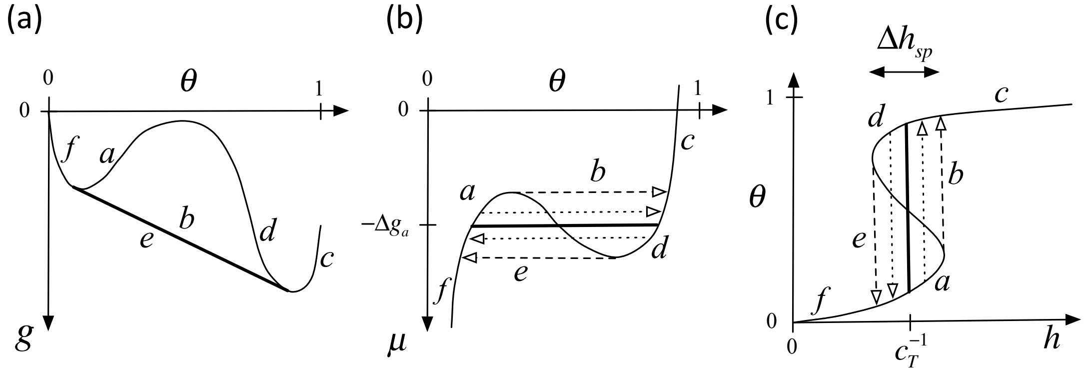

Figure 3: Effects of lateral forces on adsorption. (a) Gibbs free energy per site g versus dimensionless filling Θ of adsorbate. The homogeneous free energy g_{hom} (thin solid line) is made convex by a common tangent construction (thick solid line), which corresponds to phase separation into high and low density regions (neglecting interphasial tension). (b) Chemical potential μ per site for homogeneous (thin solid) and phase separated (thick solid) states. (c) The corresponing filling fraction versus relative humidity h for quasi-equilibrium between the adsorbate and vapor. Hysteresis during adsorption ($a \to b \to c$ in Fig. 10) or desorption ($d \to e \to f$) results from the delay in phase separation due to either nucleation (dotted lines) or spinodal decomposition (dashed lines).

where we set the zero of chemical potential in the saturated vapor phase ($h = 1$). Setting $\mu_{hom} = \mu_v$ yields the equilibrium sorption curve (Θ vs h) for homogeneous filling of the nanopore, shown in Fig. 3(c). The non-convex free energy is seen to correspond to a non-invertible sorption curve with three degenerate filling fractions over the "spinodal range" of humidities, Δh_{sp}. Over the corresponding spinodal gap of filling fractions, where the free energy loses convexity ($\frac{d^2 g_{hom}}{d\Theta^2} < 0$) and the chemical potential decreases with concentration ($\frac{d\mu_{hom}}{d\Theta} < 0$), the homogeneous adsorbate is linearly unstable with respect to the growth of infinitesimal perturbations of the concentration profile (spinodal decomposition). This leads to sorption hysteresis with varying humidity, as represented by the dashed lines in Figure 3.

It is possible for phase separation to occur for any metastable composition within the miscibility gap, but outside the spinodal gap, a sufficiently large critical nucleus of the second phase is required. In the typical case of heterogeneous nucleation, phase separation is triggered at nanopore defects or boundaries, as sketched in Figure 2. If nucleation occurs before spinodal decomposition, then phase separation occurs with less overshoot of the chemical potential plateau and smaller sorption hysteresis, as denoted by the dotted lines in Figure 3 (b) and (c), respectively. For sufficiently slow humidity variations, the nanopore should be able to reversibly follow the convex equilibrium free energy surface without any hysteresis, but depending on experimental conditions, the required nucleation and growth may not have enough time to occur. In the absence of nucleation, the spinodal humidity range Δh_{sp} provides a convenient upper bound on the equilibrium sorption hysteresis, and so we now proceed to calculate it using a simple model.

Regular Solution Model: The simplest mean-field model of adsorption with lateral forces

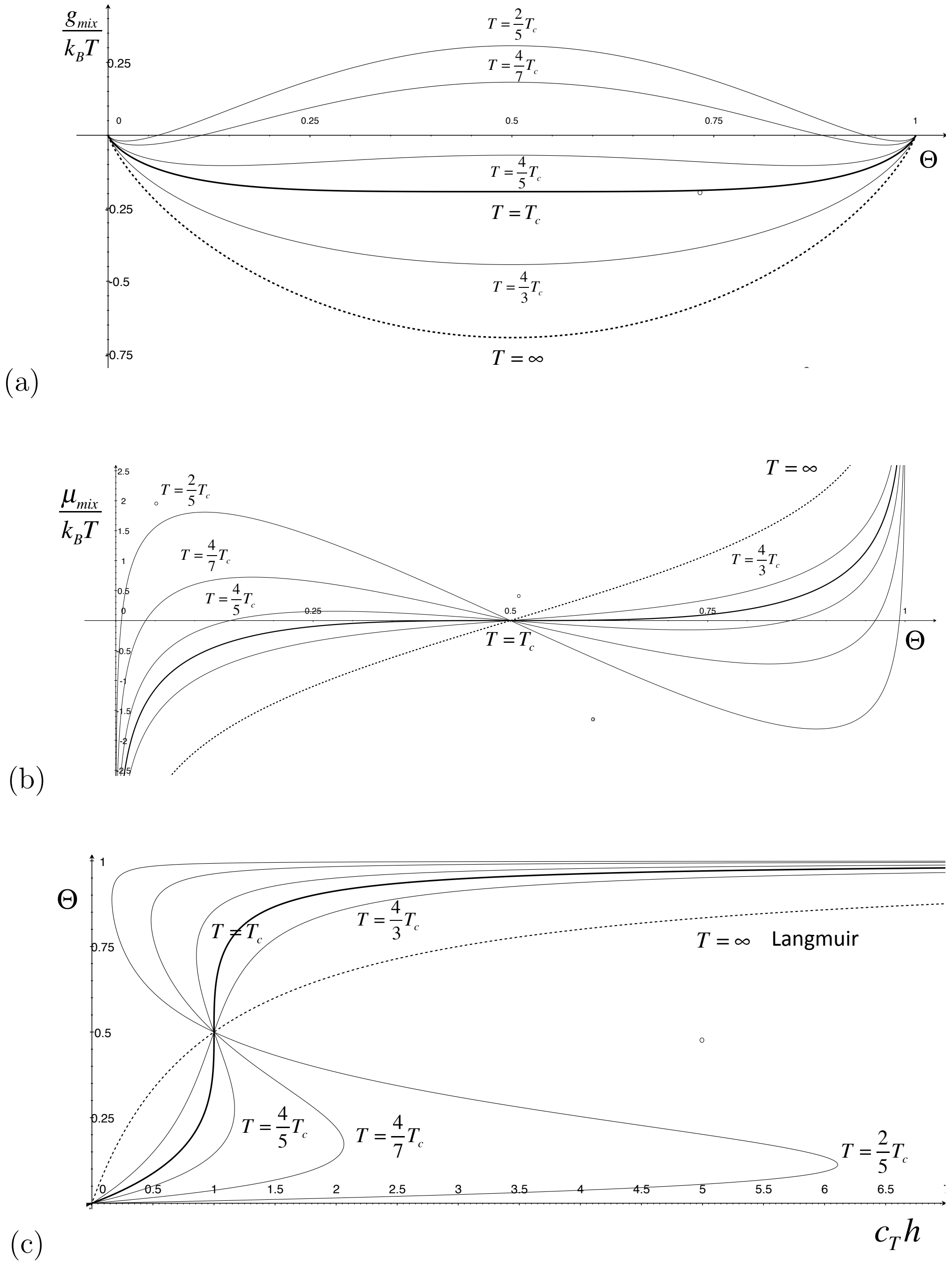

Figure 4: Thermodynamics of condensation in the regular solution model for an adsorbed monolayer with attractive intermolecular forces ($\omega > 0$). (a) Free energy of mixing versus filling fraction. (b) Homogeneous chemical potential (shifted by the adsorption free energy) versus filling fraction. (c) Filling fraction versus humidity. Below the critical temperature $T_c = \frac{\omega}{2k_B}$, enthalpy dominates entropy; the free energy is non-convex; the chemical potential is non-monotonic; and the adsorption isotherms are multi-valued, leading to hysteresis.

is the regular solution model for a binary mixture [55, 56, 59], whose free energy of mixing,

$$g_{mix} = k_B T \left[\Theta \ln \Theta + (1-\Theta)\ln(1-\Theta)\right] + \omega\Theta(1-\Theta) \tag{6}$$

comes from the continuum limit of a lattice gas of filled and empty sites. The first two terms represent the configurational entropy of particles and holes in the lattice, and the last term represents the enthalpy of mixing, expressed as a particle-hole interaction. The lattice gas could represent individual adsorbate molecules in a monolayer, either on a free surface or in a flat one-molecule-thick nanopore as in Fig. 2. As discussed below, the same model could also provide a first approximation of hindered multilayer adsorption, where the particles and holes represent coarsened molecular droplets and bubbles spanning the interior of a nanopore. Therefore, we will proceed to analyze sorption hysteresis in general terms without yet referring a specific pore geometry.

Lateral adsorbate-adsorbate forces are captured by the regular solution parameter, ω, equal to the mean energy of pairwise attraction between adsorbed molecules,

$$\omega = \int_{V_s} d\vec{r} \int_P d\vec{r}' \, \frac{1}{2}\Phi(|\vec{r}-\vec{r}'|)\, p(\vec{r}|\vec{r}') \tag{7}$$

where $\Phi(r)$ is the pair potential between adsorbate molecules, $p(\vec{r}|\vec{r}')$ is the conditional probability density of finding a molecule at $\vec{r}'$ anywhere in the pore volume P given a molecule at $\vec{r}$ in the site volume V_s. (The factor $\frac{1}{2}$ avoids double counting pair interactions.) Note that Δg_a and ω depend on position in a heterogeneous pore, whose geometry or surface chemistry varies with position.

As shown in Figure 4(a), the homogeneous free energy of mixing reflects a competition between entropy, which favors mixing ($\Theta = \frac{1}{2}$) and enthalpy, which favors de-mixing or phase separation ($\Theta = 0, 1$). At high temperature, entropy dominates, and the free energy is convex with a minimum at $\Theta = \frac{1}{2}$. Below a critical temperature,

$$T_c = \frac{\omega}{2k_B} \tag{8}$$

enthalpy (due to attractive lateral forces) begins to dominate entropy, and there is a pitchfork bifurcation (in the mathematical sense), leading to two local minima of the free energy density, corresponding to stable high-density and low-density phases. The miscibility gap is the range of metastable homogeneous compositions, bounded by the circles in Fig. 4(a). The homogeneous chemical potential is given by

$$\mu_{hom} = k_B T \ln \frac{\Theta}{1-\Theta} + \omega(1-2\Theta) - \Delta g_a \tag{9}$$

which is plotted for different temperatures in Figure 4(b) to illustrate the onset of non-monotonic behavior for $T < T_c$. The spinodal gap is the range of unstable compositions, bounded by circles in Fig. 4(b).

The corresponding adsorption isotherm, obtained by setting $\mu_{hom} = \mu_v$, is given by

$$c_T h = \left(\frac{\Theta_{hom}}{1-\Theta_{hom}}\right) \exp\left(\frac{\omega(1-2\Theta_{hom})}{k_B T}\right), \quad \text{where} \quad c_T = c_0 \exp\left(\frac{\Delta q_a}{k_B T}\right) \tag{10}$$

and plotted in Figure 4(c). At high temperature, we recover the classical Langmuir isotherm without lateral interactions,

$$\Theta_{hom} \sim \frac{c_T h}{1 + c_T h} \quad \text{for} \quad T \gg T_c. \tag{11}$$

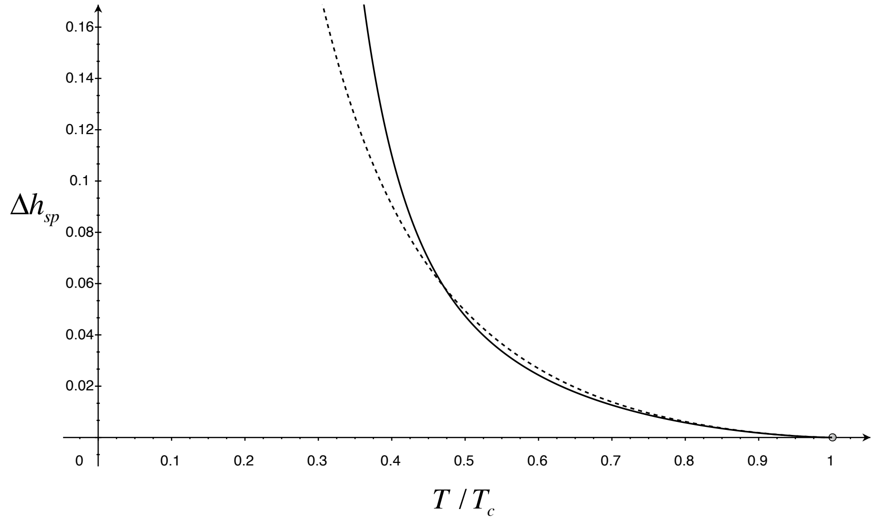

Figure 5: Simple analytical prediction of the temperature dependence of sorption hysteresis, based on the regular solution model for lateral interactions in the adsorbate. The change in relative humidity across the spinodal range Δh_{sp} is plotted against reduced temperature T/T_c, where we set $c_T = 54$ for monolayer water adsorption in cement paste or concrete. We also neglect the weak temperature dependence of c_T since adsorption forces are much stronger than lateral forces ($\Delta q_a \gg 2k_BT_c = \omega$). The exact solution (12)-(13) (solid curve) is well approximated over this range by the asymptotic power law at the critical point (14) (dashed curve). At higher temperatures, $T > T_c$, molecular condensation is thermodynamically unfavorable due to the dominance of entropy over enthalpy.

Below the critical point, $T < T_c$, the modified Langmuir isotherm with lateral interactions becomes non-monotonic, and the sorption curve exhibits hysteresis.

The spinodal humidity range, which provides an upper bound on the humidity hysteresis in this model, can be derived analytically:

$$\Delta h_{sp} = \frac{2}{c_0} f\left(\frac{T_c}{T}\right) \exp\left(-\frac{\Delta q_a}{k_BT}\right) \tag{12}$$

where the Arrhenius temperature dependence is augmented by a prefactor

$$f(u) = \frac{c_T\,\Delta h_{sp}}{2} = (2u-1)\sinh v - v\cosh v, \quad \text{where} \quad v = 2\sqrt{u(u-1)}, \;\; u = \frac{T_c}{T} = \frac{\omega}{2k_BT}. \tag{13}$$

An important prediction of this model is that *sorption hysteresis decreases with increasing temperature and vanishes as a power law at the critical point:*

$$\Delta h_{sp} \sim \frac{8}{3c_T}\left(\frac{T_c}{T} - 1\right)^{3/2} \quad \text{as } T \to T_c, \tag{14}$$

The same $\frac{3}{2}$ critical exponent also arises in the temperature dependence of the interfacial tension between the low-density and high-density phases in the van der Waals theory of capillarity [87] and the related Cahn-Hilliard model of phase separation [56], which we consider in the next section. (In structural mechanics, this scaling relation is analogous to Koiter's 2/3-power law for the difference between the critical load at symmetric bifurcation of a perfect structure and the stability limit of imperfect structures with vanishing imperfections [10]. There is also Koiter's 1/2-power law for the bifurcation of a perfect system that is asymmetric, and we would expect analogous scaling, $\Delta h_{sp} \propto (T_c - T)^2$ in a different model with broken symmetry in the entropy and/or enthalpy density around $\Theta = \frac{1}{2}$.) More generally, the theory of critical phenomena provides many ways for nontrivial power law scalings to arise, $\Delta h_{sp} \propto (T_c - T)^\nu$, and the exponent ν is best determined by experiment for a given material.

As shown in Figure 5, the critical power law (14) is a good approximation of the exact formula (12)-(13) over a broad temperature range corresponding to typical hysteresis values, $\Delta h < 10$. In these formulae, the weak dependence of c_T on temperature can be neglected if orthogonal adsorption forces are much stronger than lateral intermolecular forces, $\Delta q_a \gg 2k_B T_c = \omega$, which is always the case whenever there is significant adsorption from the vapor. (Otherwise, bulk liquid condensation would occur before surface adsorption.) For water adsorption in cement paste or concrete, this assumption is consistent with an early estimate of $\Delta q_a / k_B = \Delta Q_a / R = 2700$ K [47], which is likely to be much larger than T_c, as discussed below (see also [48], p. 210).

In such cases, the dominant temperature dependence in (12) comes from the prefactor (13), which vanishes at the critical point. Physically, sorption hysteresis disappears above the critical temperature because entropy, which promotes uniform surface coverage, then dominates the enthalpy of lateral interactions, which promotes molecular condensation. This is a very general effect, which will also arise in more complicated models (e.g. for multilayer adsorption [52, 51, 49, 50]), as long as the lateral interactions among adsorbed molecules are attractive.

Molecular Condensation on Bounded Surfaces

Interphasial Tension: The foregoing theory describes sorption hysteresis for an infinite pore or surface, since it considers only the homogeneous free energy per site. In a finite system, phase separation is hindered by the interfacial (or "interphasial") tension between immiscible stable phases, below the critical temperature. The standard mathematical model of interphasial tension is based on the concept of a diffuse interface of continuously varying density, first introduced by Van der Waals in his original "thermodynamic theory of capillarity" [87] and still used today to describe surface wetting by thin liquid films [81, 84, 88, 85]. The same model has also been used to describe disjoining pressure in liquid-filled nanopores [86], albeit without making connections to adsorption isotherms and sorption hysteresis in nanoporous solids. Modern interest in this approach and many subsequent extensions sprang from the celebrated paper of Cahn and Hilliard [56], which used the regular solution model to rederive and extend key results of Van der Waals [87] and paved the way for phase-field models in materials science [58, 59].

Given the homogeneous free energy (1) per discretized pore volume $V_s(\vec{r})$ (associated with fixed sites on the nearby pore surface), the total free energy G of an arbitrary (possible multiply connected) pore geometry can be expressed as an integral over the pore volume,

$$G[\Theta, S] = \int d\vec{r} \left[g_{hom}(\Theta, \vec{r}) + \frac{1}{2} \nabla\Theta \cdot \boldsymbol{K}(\vec{r}) \nabla\Theta \right] \tag{15}$$

which is a functional of $\Theta(\vec{r})$, the dimensionless filling fraction of the volume $V_s(\vec{r})$ (e.g. measured in monolayers, and possibly larger than one for a site volume spanning a nanopore) and

$S(\vec{r})$, a function prescribing the surface geometry of the pore (e.g. via a level-set or phase-field description). The coefficient $\boldsymbol{K}$ in the second term is the "gradient penalty tensor", which approximates corrections to the free energy density due to density variations, as well as the interphasial tension (see below). In principle, both g_{hom} and $\boldsymbol{K}$ depend on position within the pore geometry specified by S. In Eq. (15), we neglect the mechanical energy stored in the solid phase [58, 62, 70], in order to emphasize our prediction that hysteresis can occur in nanoporous solids whose mechanical deformation, if any, is too small to affect the equilibrium distribution of the adsorbate. It would be straightforward to incorporate mechanical response of the solid matrix in a more sophisticated model, e.g. following Ref. [70].

The diffusional chemical potential is given by the functional derivative with respect to composition,

$$\mu = \frac{\delta G}{\delta \Theta} = \mu_{hom} - \nabla \cdot \boldsymbol{K} \nabla \Theta \tag{16}$$

where $\mu_{hom} = g'_{hom}$ is the homogeneous chemical potential (4). Physically, this corresponds to the free energy change upon creating a continuum "molecule" represented by a delta function at $\vec{r}$. Outside the spinodal range, setting chemical potential $\mu =$ constant yields one uniform solution, corresponding to a stable homogeneous phase. Within the spinodal range, there are three uniform solutions, two stable and one unstable, and $\mu =$ constant yields a Beltrami differential equation, whose nontrivial solution corresponds to a phase separated system with a diffuse phase boundary. In the regime of strong phase separation $\omega \gg k_B T$ or $T \ll T_c$, the width λ of the phase boundary scales as

$$\lambda = \sqrt{\frac{K}{\omega}} \tag{17}$$

in each eigendirection of the $\boldsymbol{K}$ tensor, and the corresponding interphasial tension (energy/area) is

$$\gamma = \rho_s \sqrt{K\omega} \tag{18}$$

where ρ_s is the density of sites per volume, or the inverse of the single-site volume [56, 69].

Suppressed Condensation in Small Pores: The tendency for phase separation is reduced in small systems, as the phase interface area to bulk volume ratio increases. More precisely, both the spinodal range [72] and miscibility gap [79, 80, 69] shrink and ultimately disappear, as the system size becomes comparable to the phase boundary thickness. For phase separation in solid materials, if the two phases have different equilibrium volumes, then elastic coherency strain energy further reduces the miscibility and spinodal gaps and can eliminate phase separation [70].

The suppression of phase transformations with decreasing system size is a universal phenomenon, which is drawing attention in other fields and has important technological applications. For example, it controls the "ultimate fineness", or minimum feature size, of polymer-in-polymer microdispersions [79, 80]. Recently, it has also played a major role in the development of high-rate Li-ion batteries using lithium iron phosphate ($\mathrm{Li}_x\mathrm{FePO}_4$), which has a strong tendency for phase separation into Li-rich and Li-poor domains. Ironically, when it was first explored as an insertion cathode material in microparticle form, $\mathrm{Li}_x\mathrm{FePO}_4$ was predicted to be good for "low power applications" as a result of slow phase separation dynamics and related mechanical deformations [73], but today, in nanoparticle form, it is capable of ultrafast battery discharge (in tens of seconds) while maintaining long cycle life [74]. In addition to size-dependent diffusivity [75], the main reasons that "nano is different" may be the shrinking of the miscibility gap [61, 62, 69, 63, 70] and the dynamical suppression of phase separation [76, 67, 70]. Analogous phenomena must also occur for vapor sorption in nanopores, as we now explain.

Consider a homogeneous adsorbate $\Theta = \Theta_0$ in a straight pore or flat surface whose longest lateral dimension is L. For example, in the case of a perfect cylindrical pore, we set L equal to the maximum of its length and diameter. This state will be linearly stable to sinusoidal perturbations of wavevector $\vec{k}$, given by $\Theta(\vec{r}) = \Theta_0(1 + \epsilon e^{i\vec{k}\cdot\vec{r}})$, if the perturbation increases the chemical potential, which implies

$$\frac{\partial \mu_{hom}}{\partial \Theta}(\Theta_0) + \vec{k} \cdot \boldsymbol{K}\vec{k} > 0 \tag{19}$$

The second term is strictly positive, so in an infinite system, where arbitrarily long wavelength perturbations ($k \to 0$) with vanishing gradient energy are possible, the spinodal range is defined by setting the first term to zero, as above. In a finite system, however, there is a minimum wavelength for perturbations set by the boundary conditions, e.g. given by $k_{min} = \frac{\pi}{L}$ for constant concentration boundary conditions, reflecting adsorption equilibrium at the farthest ends of the pores. As a result, the spinodal range of unstable compositions, determined by $\mu < 0$, is generally reduced [72, 79, 69].

The corresponding spinodal humidity range $\Delta h_{sp}(L)$, defined as the jump in the homogeneous isotherm humidity between the spinodal points satisfying $\mu(\Theta, L) = 0$, is given by the same formula as derived above, Eqs. (12)-(13), but only with a length-dependent critical temperature,

$$T_c(L) = T_c^\infty \left(1 - \frac{\pi^2\lambda^2}{2L^2}\right), \quad \text{where} \quad T_c^\infty = \frac{\omega}{2k_B}. \tag{20}$$

The critical point is depressed as the ratio of the system size to the phase boundary thickness $\frac{\lambda}{L}$ decreases. For very small systems, $L < L_c = \frac{\pi\lambda}{\sqrt{2}}$, the critical temperature vanishes, and the homogeneous state is linearly stable, even at zero temperature. In simple physical terms, molecular condensation is only possible on surfaces whose length L is large enough to accommodate an equilibrium phase boundary of thickness λ.

Enhanced Hysteresis in Small Pores: One might expect hysteresis to be suppressed in short pores, due to the reduced spinodal and miscibility gaps, but this is not the case since it is the humidity, not the filling fraction, that is experimentally controlled. The basic physics is sketched in Figure 6. First consider the possibility of nucleation, where the second phase is created by fluctuations over the surface or at defects or pore edges. As the pore size is decreased, there are fewer sites for nucleation, and the reduced nucleation probability enhances hysteresis by preserving the homogeneous state as the humidity is varied. Even if nucleation is very fast, the reduced miscibility gap Δh_{hom}^L increases the corresponding humidity range of hysteresis, up to the limit set by Δh_{sp}^∞.

In the absence of nucleation, phase separation must occur by spinodal decomposition, which is also suppressed in short pores. If the humidity passes out of the spinodal range, then the adsorbate can pass into the infinite-system spinodal gap Δh_{hom}^∞ while remaining uniform. After the overshoot, it experiences a strong thermodynamic driving force to vary the concentration until the new homogeneous equilibrium state is reached, and phase separation may not have enough time to occur during this sudden transition. (This non-equilibrium transition state has recently been called a "quasi-solid solution" [67].) As a result, the infinite-system spinodal humidity range, $\Delta h_{sp}^\infty(T)$, given by Eqs. (12)-(14), provides a robust estimate of sorption hysteresis in finite-length pores of any size if nucleation is too slow to occur over experimental time scales.

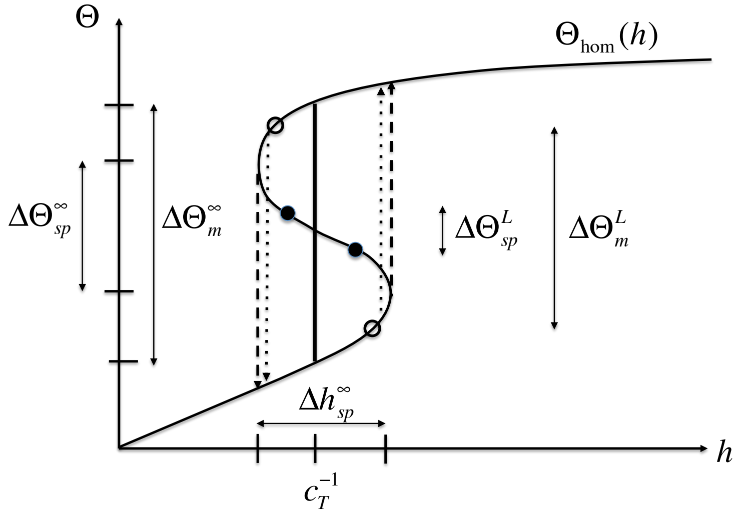

Figure 6: Molecular condensation on a bounded surface of maximum dimension L (e.g. length or diameter of a cylindrical pore), where humidity h is controlled (rather than the mean filling fraction Θ). If nucleation is possible, then, as the miscibility gap $\Delta\Theta_m^L$ shrinks (open circles) and the nucleation rate decreases with decreasing pore size, the hysteresis (dotted lines) increases up to the maximum set by the spinodal humidity range, Δh_{sp}^{∞}. (b) In the absence of nucleation, the adsorbate undergoes sudden transitions at the infinite-system spinodals (dashed lines), prior to reaching the reduced spinodal gap $\Delta\Theta_{sp}^L$ (black points).

Molecular Condensation in Single Nanopores

Theory of Hindered Multilayer Adsorption: A general continuum model of adsorption in nanoporous media of arbitrary geometry could be based on the van der Waals (or Cahn-Hilliard) model, Eq. (15), where $\Theta(\vec{x})$ is the local mean density of the adsorbate at a point in the pore. The main difference with monolayer adsorption is that the adsorption free energy $\Delta g_a(\vec{x})$ would depend on $\vec{x}$ and reflects the decay of surface forces with distance from the pore walls, including screening effects due to the other molecules. The local interaction energy, $\omega(\vec{x})$, would also depend on position, approaching a bulk value as the influence of surface forces decays with distance from the nearest wall. The gradient penalty $K(\vec{x})$ would represent the local free energy difference associated with broken or frustrated molecular bonds (the nanoscale analog of gas-liquid surface tension), and this, too, would generally depend on position.

The dynamics of the concentration profile in such a model would be described by the Cahn-Hilliard equation [59, 89],

$$\frac{\partial\Theta}{\partial t} = \nabla \cdot [M\Theta\nabla\mu] \tag{21}$$

where the chemical potential $\mu(\Theta, \vec{x})$ is given by (16) and the diffusional particle mobility $M(\Theta, \vec{x})$ generally depends on the concentration and position. For example, in the foregoing regular solution model for the first monolayer, the mobility should be proportional to the free volume, $M = M_0(1 - \Theta)$ (this effect was omitted in early models and yields a "modified Cahn-Hilliard equation" [89]). More generally, to account for finite pores, one should use the "Cahn-Hilliard-Reaction model", which includes thermodynamically consistent boundary conditions for molecules to enter and leave the pore space [68, 69]. It is beyond the scope of this paper to analyze or simulate the intrapore adsorbate distribution in detail, but this

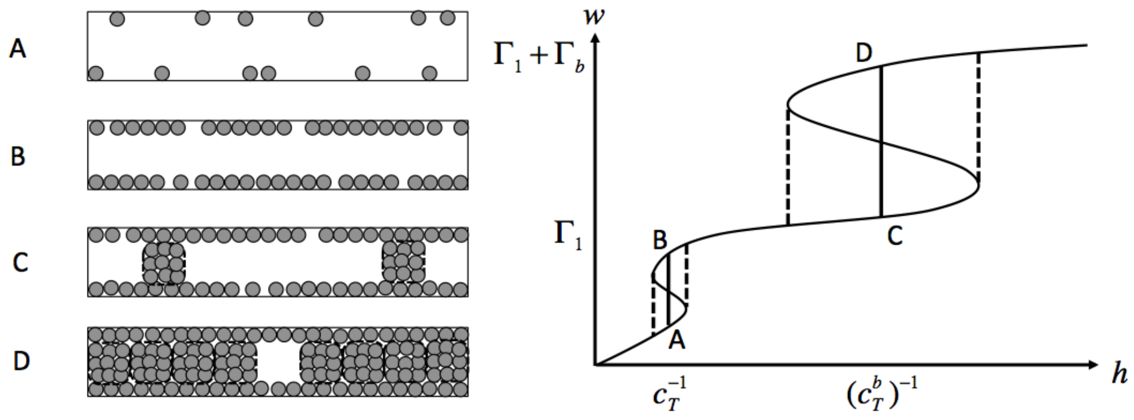

Figure 7: Hierarchical wetting model for hindered multilayer adsorption in nanopores. The homogeneous isotherm, as in Eq. (22), exhibits two regions of hysteresis: (i) a small loop at low vapor pressure for low-density (A) and high-density (B) phases in the first monolayer and (ii) a larger loop at higher vapor pressure for the low-density (C) and high-density (D) phases of coarsened pore-spanning droplets and bubbles in the bulk fluid, outside the monolayer.

would be interesting to pursue in future work. Such a nanoscale, statistical continuum model may be able to capture key features of molecular dynamics simulations [18, 19, 20, 22, 23, 21] at greatly reduced computational cost, thereby allowing extensions to experimental time and length scales.

Hierarchical Wetting Model: We proceed instead by making some simple approximations to enable us to predict general features of molecular condensation in nanoporous media. It is often reasonable to assume that in the first monolayer there are strong surface forces, which decay quickly with distance from the surface. In case of concrete, for example, water adsorption in C-S-H nanopores containing dissolved salts involves strong electrostatic forces, which are screened at the molecular scale due to diffuse charge, solvated ion crowding and electrostatic correlations [77, 78]. For simplicity, let us assume that the regular solution model above describes the mean homogeneous coverage $\Omega_{hom}(h, T; c_T, \omega)$ of the first monolayer on the surface at low vapor pressure. Here, c_T and ω describe the local adsorption and interaction energies, which could depend on surface heterogeneities or curvature in very small pores. In thick pores at low vapor pressure, the dynamics of the concentration profile in the first monolayer could be described by the Allen-Cahn equation [59] for an open system (or its generalization for nonlinear adsorption kinetics [67]), since gas molecules are freely exchanged with the adsorbate at all points.

Here we consider what would happen in the general case of nanopores, which are thick enough to be covered by non-overlapping monolayers at low vapor pressure, but thin enough to be spanned by a condensed liquid phase at moderate vapor pressures (below the saturation pressure). Over experimental time scales (e.g. minutes to months), the Cahn-Hilliard equation predicts that small clusters of molecules or voids resulting from thermal fluctuations of the homogeneous state will coarsen within the nanopores, so as to minimize the gradient energy (which is the molecular analog of surface tension). Assuming strong wetting in the first monolayer, this coarsening proceeds until the size of the separated nanophases is set by the diameter of the bulk region just outside the first monolayer.

In that case, as a crude first approximation, we describe the bulk region by another regular solution model, whose characteristic lattice size is that of the pore bulk. The filling fraction of the bulk region is thus given by $\Theta_{\mathrm{hom}}(h, T; c_T^b, \omega^b)$, where $c_T^b = \exp(\Delta g_a^b/k_B T)$ and ω^b are effective values for molecular droplets in the pore. The total weight of a homogeneous adsorbate in the pore is then given by

$$w_{hom}(h, T) = \Gamma_1 \Theta_{hom}(h, T; c_T, \omega) + \Gamma^b \Theta_{\mathrm{hom}}(h, T; c_T^b, \omega^b). \tag{22}$$

where Γ_1 is the total weight of a full surface monolayer and Γ^b is the weight of the filled bulk region. This "Hierarchical Wetting" model is surely oversimplified, but it captures typical results of molecular dynamics simulations [20, 22, 23, 21] and allows considerable insight into experimental data, as we now explain.

Surface versus bulk phase separation in nanopores: This very simple model leads to two types of hysteresis, one due to the condensation of adatom clusters in the first monolayer at low vapor pressure and the second due to the condensation of pore-spanning clusters of molecules or voids ("nanodroplets" and "nanobubbles", respectively) in the bulk pore at higher vapor pressure. Each hysteresis has its own magnitude and critical temperature. If the pore radius is R and monolayer thickness, a, then the effective interaction parameter scales with the geometrical ratio:

$$\frac{\omega^b}{\omega} \approx \frac{T_c^b}{T_c} \approx \frac{\Delta h^b}{\Delta h} \approx \frac{R}{a}, \tag{23}$$

which is typically larger than one, except in molecular scale pores (which might not be macroscopically accessible). An interesting implication is that critical temperature T_c^b for droplet phase separation in the bulk nanopore is larger from that of the first monolayer T_c by the same factor α. Well below the critical temperatures, the magnitude of the bulk hysteresis Δh^b (dominated by enthalpy) is also larger than that of the surface layer Δh, by the same factor. Bulk hysteresis is also shifted to larger humidities in the multilayer adsorption regime, assuming that the adsorption energy in the bulk is much less than it is at the surface, $\Delta g_a^b \ll \Delta g_a$.

These simple concepts are illustrated in Fig. 7. As the nanopore is emptied and filled, there are two instabilities corresponding to sudden phase separation in the first monolayer, at low vapor pressure, and in the bulk, at higher vapor pressure. The resulting desorption and sorption isotherms for this crude model already resemble the experimental data for concrete or cement paste at room temperature in Fig. 1. The theory also qualitatively predicts a nontrivial effect of temperature, which suppresses hysteresis in the monolayers at low vapor pressures more than in the bulk pores at higher vapor pressures.

Snap-Through Instabilities: The reader may be wondering how our general statistical thermodynamic theory in Part II relates to the snap-through instabilities predicted for nonuniform pore openings in Part I. One major difference is that the theory of Part I does not account for the entropy of molecular rearrangements in the adsorbate and thus is mainly relevant for low temperature, where enthalpy dominates and sorption or desorption proceeds sequentially through the junction, like a crack tip. In the present model, phase separation can occur anywhere in the system that achieves a locally metastable state, and thus the sorption or desorption process can effectively tunnel through a junction. Nevertheless, a junction between two nanopores of different geometry or surface chemistry can act as a barrier for snap-through instabilities, due to the interfacial tension associated with lateral interactions across the junction.

To model the pinning effect of molecular interactions at junctions, we use again the Cahn-Hilliard (or Van der Waals) model (15), but it suffices to average over the cross section and focus on density gradients through the junction or pore opening. Relative to the free energy of an infinite system, the gradient energy per area (i.e. the interphasial tension at the junction) can be approximated as

$$\Delta G_i \approx \lambda K \left(\frac{\Delta\tilde{\Theta}}{\lambda}\right)^2 \approx \omega^b\, \Delta\tilde{\Theta}^2 \tag{24}$$

where λ is the local interface width and $\tilde{\Theta} = \Theta/\Theta_{max}$ is the jump in dimensionless adsorbate density, or total filling fraction ($0 < \tilde{\Theta} < 1$). This additional energy barrier must be overcome for phase separation to occur across the junction. Just as in the foregoing case of short pores, the interphasial tension can lead to hindrance or even suppression of phase separation.

When phase separation does occur across the junction, the chemical potential jumps according to Eq. (16) and causes an increase in humidity hysteresis at a given mean weight, due to the need to overcome the interfacial energy at the junction. As shown in Figure 8 for the heterogeneous pore geometry in (a), this effect can be estimated graphically using Eq. (24) by plotting in (c) the two homogeneous isotherms as the dimensionless filling fraction $\tilde{\Theta}$ versus humidity h and measuring the density difference $\Delta\tilde{\Theta}$ between the two curves as the humidity is varied. The filling fraction jumps are also evident in the density profiles across heterogeneous pore in (d). The interfacial contribution to hysteresis at each junction, ΔG_i, which leads to the enlarged hysteresis in (d), can be of comparable magnitude to the intrinsic hysteresis for the interior of the pore, ω^b, since each results from the energy of lateral forces in a cross section of the pore. As the interfacial energy builds up during sorption, the humidity is gradually amplified by $\exp(\Delta G_i/k_BT)$, while during desorption the humidity is multiplied by $\exp(-\Delta G_i/k_BT)$. The net effect is to widen the hysteresis envelope associated with each phase separation process, e.g. in the first monolayer and the two types of bulk pores.

The sorption/desorption sequences predicted by these arguments using the simple Hierarchical Wetting Model are similar to those observed in molecular dynamics simulations of wetting fluids in heterogeneous nanopores by Coasne, Pellenq and collaborators [20, 22, 23, 21]. The example shown in Figure 8(a) consists of a series of multilayer-thick pores of two different radii a and b, which terminates at the free surfaces of much larger pores. The bulk regions of the thicker b pores have smaller adsorption energy Δg^b (larger c_T^{-1}) and larger interaction energy ω^b for spanning nanodroplets and nanobubbles than those of the thinner a pores. This leads to the different rescaled isotherms $\tilde{\Theta}(h)$ for a and b sections plotted in (c), which allow the sorption/desorption sequences to be predicted. During sorption starting from very low humidity, a monolayer first covers the entire pore surface in state A, and then bulk molecular condensation proceeds to the narrower sections in state B, followed by the thicker sections in state C. The corresponding spatial profiles of the filling fraction are shown in (d), from which the interfacial energies at the junctions can be estimated using Eq. (24). Due to the larger density jump at the pore ends, there is a larger interfacial energy there, compared to the internal a/b junctions, and this can cause condensation to occur in outermost pores after the others, leading to intermediate states B' and C' shown in (a).

Solid Matrix Deformation: Although we emphasize the statistical thermodynamic origin of sorption hysteresis, mechanical deformation of the solid matrix during phase separation could play an important role, even in the absence of pore collapse. Molecular condensation events lead to sudden changes in disjoining (or joining) pressure, which can influence neighboring pores, perhaps even triggering chains of subsequent phase separation events, as stresses are quickly transmitted through in the solid (at the local speed of sound). Analogous effects of "coherency strain" due to adsorption in elastic crystal lattices have recently been considered in Li-ion batteries and shown to contribute to suppression of phase separation and nonlinear

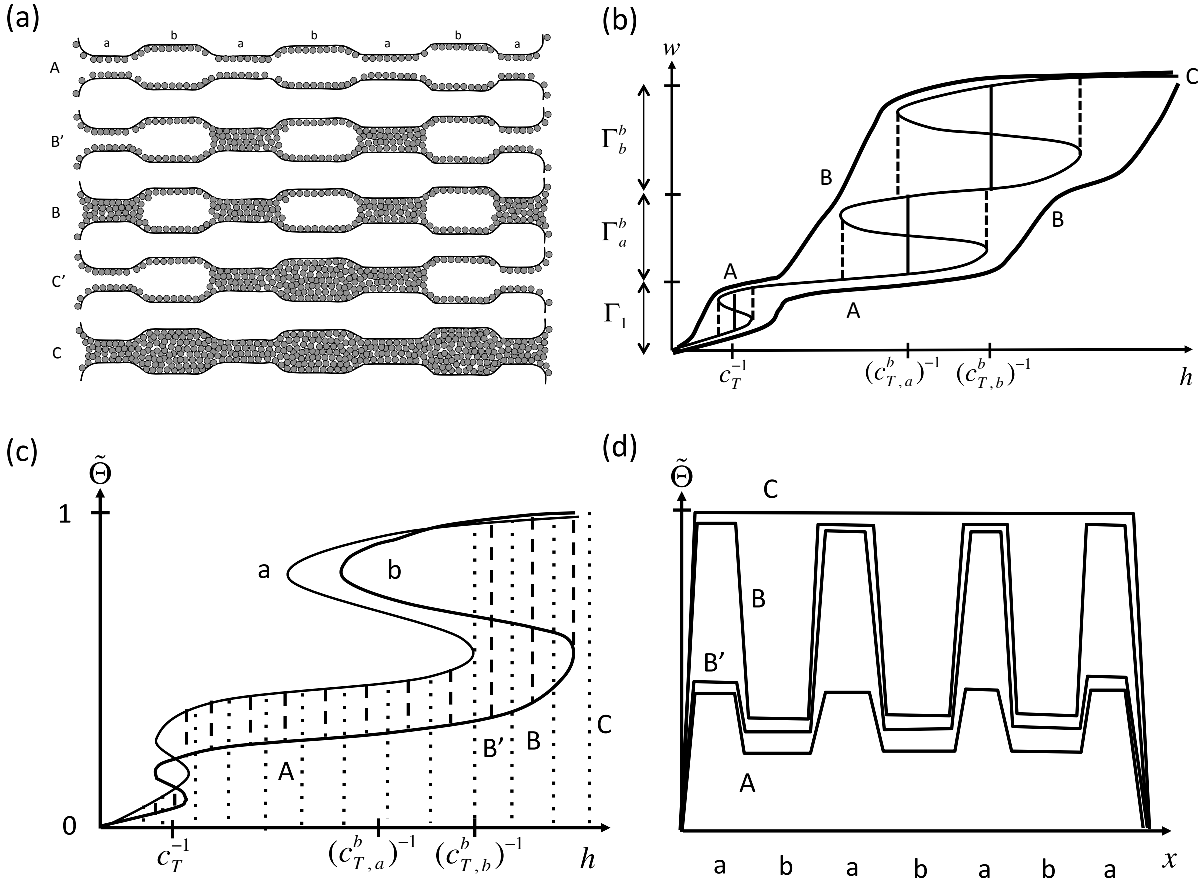

Figure 8: Molecular condensation in a heterogeneous multilayer nanopore with sections a and b of two different thicknesses. (a) Typical molecular configurations A, B, B', C, and C' at different stages of sorption. (b) Net sorption and desorption isotherms for the nanopore including interfacial energies with the states A, B, and C indicated. (c) Isotherms of dimensionless filling fraction $\tilde{\Theta}$ (mean density) versus relative humidity h for the a and b sections of the pore, showing the jumps at a/b junctions (dashed lines) and the empty regions at the pore ends (dotted lines). (d) Spatial density profiles, $\tilde{\Theta}(x)$, for the states in part (a), where the interfacial energy due to each jump, which enhances the hysteresis in (b), scales as $\omega^b \Delta\tilde{\Theta}^2$.

pattern formation, consistent with experimental observations [70]. Ultimately, a complete model of sorption dynamics in nanoporous solids should take into account viscoelastic relaxation, or even plastic deformation and damage to the solid matrix, coupled to molecular condensation and transport.

Molecular Condensation in Nanoporous Solids

Mosaic Instability: It is important to emphasize that quasi-equilibrium phase separation across a nonuniform network of pores need not be sequential, as suggested in Part I based on mechanical analogies. As long as there is sufficient time for the chemical potential to equilibrate across the pore network between tiny, applied steps in humidity, then there is no prescribed order for the intermittent events of filling or emptying in different pores. At the macroscopic scale, the resulting "mosaic instability" of discrete molecular condensation events in different, tiny nanopores manifests itself by accumulating many incremental sorption/desorption isotherms into a smoother overall curve, as shown in Figure 9. This effect has recently been invoked to explain the noisy thermodynamic hysteresis of voltage versus state of charge in phase-separating nanocomposite Li-ion battery cathodes [65, 66].

This approximation inevitably breaks down, however, in sufficiently large porous bodies, where the transport of mass or heat is too slow to fully equilibrate the system between external humidity steps. In such cases, the progression of phase separation is biased by transport limitations and indeed behaves like a sequence of snap-through instabilities propagating through the porous medium, starting from the edges where the humidity is controlled. Analogous phenomena have also recently been predicted [71] and observed [64] in Li-ion batteries, where a narrow front of mosaic instability can propagate across the electrode from the separator, limited by diffusion of lithium ions in the electrolyte. Similar dynamical phase separation phenomena must occur during vapor sorption/desorption in porous media, but to our knowledge no simple theory is yet available for the resulting macroscopic dynamics. Percolation concepts, which have been applied to sorption hysteresis due to classical capillarity in pore networks [53], may be useful, but molecular condensation, gas transport and adsorption reaction kinetics should also be considered. Analyzing the macroscopic dynamics of sorption and desorption in phase separating nanoporous solids would be a very interesting avenue for future research.

Rate Dependence. Non-equilibrium phenomena always play a role in hysteresis, no matter how slowly experiment is performed. Whenever transport or adsorption kinetics are at least partly rate limiting, there will be an additional non-thermodynamic contribution to hysteresis, sketched in Fig. 9(b), which is related to the work done (or frictional energy dissipated) to drive the system, as noted in Part I. The faster the humidity sweep rate, the larger the hysteresis, in excess of the thermodynamic contribution described above. This effect is analogous to the "overpotential" or "internal resistances" observed in battery cycling under different conditions. For example, galvanostatic discharge is analogous to constant mass flux dw/dt, and more realistic situations for gas sorption, such as small humidity steps Δh or constant rate of humidity variation dh/dt, are analogous to potentiostatic intermittent titration and cyclic voltammetry, respectively. In principle, detailed mathematical modeling of transient vapor sorption/desorption taking into account transport, adsorption kinetics and phase separation could enable quantitative information about the material to be extracted from the rate-dependence of the observed hysteresis.

Temperature Dependence. As noted above, the very simple Hierarchical Wetting Model already makes an interesting prediction about the temperature dependence of hysteresis

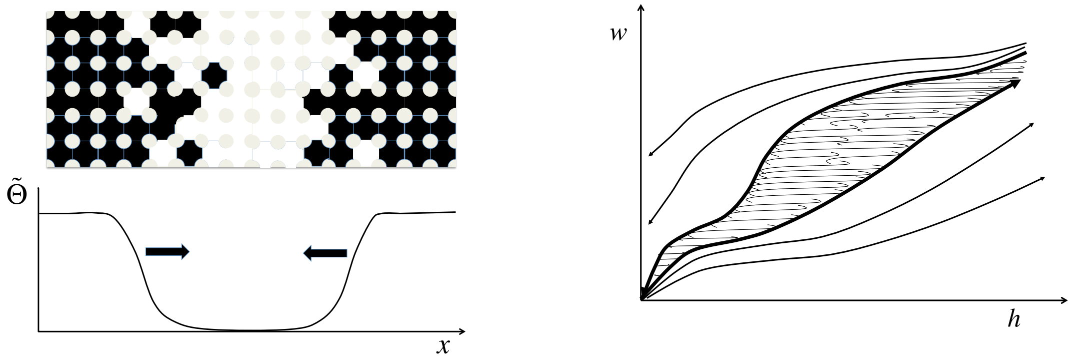

(a) (b)

Figure 9: Molecular condensation in macroscopic nanoporous solids. (a) Discrete nanopore transformations due to local mosaic instabilities propagate across the material in a narrow front from the edges where the vapor pressure is controlled. The front thickness scales with sweep rate dw/dt, and at high rates spans the system. (b) Sorption hysteresis due to quasi-equilibrium thermodynamics (thick solid lines) corresponding to countless, tiny condensation events (thin interior curves) for individual nanopores. With increasing sweep rate, there is additional non-thermodynamic hysteresis (thin exterior curves) due to internal resistances to transport and/or adsorption reaction kinetics.

in nanoporous solids with strong wetting. As sketched in Figure 10, hysteresis is pronounced at low temperature and disappears at high temperature, but there is an intermediate range of temperatures ($T_c < T < T_c^b$) where hysteresis vanishes at low vapor pressure (monolayer filling) but persists at high vapor pressure (bulk nanopore filling). In complicated nanoporous geometries, the general effect should remain: As the temperature is increased, hysteresis vanishes first at low vapor pressure in the monolayer regime and then at high vapor pressure in the bulk nanopore regime. The reason is that the effective interaction energy ω^b of pore-spanning nanodroplets and nanobubbles is larger than that of individual adsorbed molecules, due to the larger number of intermolecular bonds. Similar arguments apply to the interfacial energy ΔG_i at a nanopore junction, which is larger at high filling than for monolayer coverage. As a result, the critical hysteresis temperatures for different bulk nanopores are larger than for monolayers.

Re-interpretation of Experimental Data for Concrete:

As noted above, water sorption hysteresis at low humidity in concrete has long been attributed to pore collapse, in spite of the lack of any testable theory. It is noteworthy, therefore, that a number of puzzling experimental observations can be explained for the first time by molecular condensation without invoking any changes in the pore structure. In some cases, our predictions seem to be quantitatively consistent with the data, although more systematic experiments and detailed modeling should done, e.g. at different temperatures and humidity sweep rates, to further test the theory.

- **Inert gas versus water vapor.** No sorption hysteresis is observed for inert gases, such as nitrogen, in the same concrete samples that exhibit large hysteresis for water

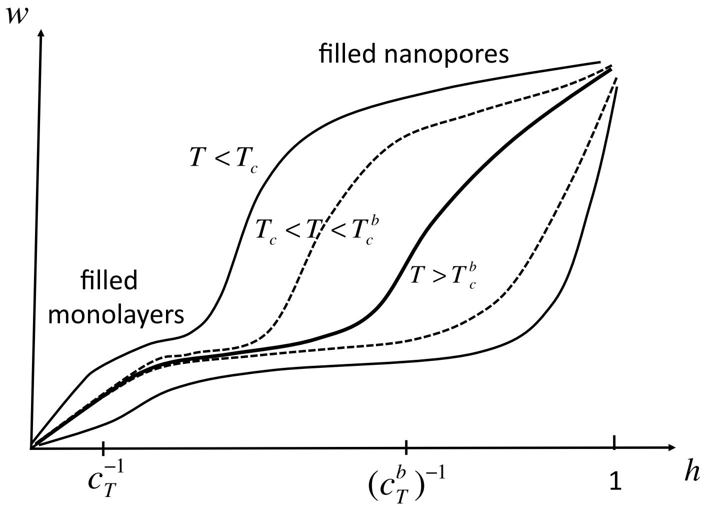

Figure 10: Temperature dependence of sorption hysteresis in nanoporous solids with strong wetting. At low temperature, pronounced hysteresis exists at all vapor pressures (thin solid curves). Above the critical temperature T_c for phase separation in a monolayer, hysteresis disappears at low vapor pressure, but remains at high vapor pressure (dashed curves) until the critical temperature for bulk nanopore phase separation, T_c^b, is exceeded (thick solid curve).

vapor [44], and our model is able to attribute this effect to differences in lateral forces. Sorption experiments are usually carried out at room temperature, which is larger than the critical temperature T_c in our model (8), if the mean pair interaction energy ω is smaller than $2k_BT = 52$ meV. This is a reasonable upper bound for the weak lateral van der Waals forces in adsorbed inert gases, and so negligible hysteresis can be expected. In contrast, adsorbed water molecules have much stronger attractive forces, leading to room-temperature hysteresis, as explain next.

- **Hysteresis at low vapor pressure.** Our theory, although oversimplified, predicts hysteresis of a reasonable scale for monolayer water sorption at room temperature. Naively, we might estimate ω by the hydrogen bond enthalpy in bulk liquid water of 23.3 kJ/mol [46], which would imply $T_c = 1380$ K, but this grossly overestimates the lateral pair interaction energy of adsorbed water molecules. A recent molecular dynamics study of water monolayers on hydrophilic silica surfaces has shown that 90% of the water molecules are "non-wetting", having much stronger bonds with the surface than with other water molecules [45]. If we work backwards from our result in Figure 5, then 1% hysteresis (in relative humidity) at room temperature implies $T_c = 410$K or $\omega = 6.8$ kJ/mol, while 10% hysteresis implies $T_c = 660$K or $\omega = 11$ kJ/mol. These are reasonable lateral interaction energies for adsorbed water molecules, which could quantitatively explain the observed hysteresis without any pore collapse.

- **Hysteresis at moderate vapor pressure.** In the regime of multilayer adsorption, we predict that the scale of hysteresis Δh^b is larger than in the monolayer regime Δh, very roughly scaling as the ratio of bulk pore radius to the monolayer thickness. This is consistent with the larger hysteresis that is always observed in the multilayer region [44]. It may even be possible to make quantitative connections with pore geometry, since the

C-S-H pores and wetting layers in cement paste are indeed at the scale of 3–10 molecular diameters, as suggested by the hysteresis ratio.

- **Temperature dependence.** We predict that sorption hysteresis should decrease with increasing temperature, although we are not aware of any prior theoretical predictions or systematic experimental studies of this effect. In a recent study [44], the hysteresis of water sorption in concrete at low vapor pressure (first monolayer) was negligible at 44°C but quite significant at 23°C, albeit in different concrete specimens, as shown in Fig. 1(a) and (b) respectively. The first adsorption isotherm was also steeper at 44°C than at 23°C (Figs 3a and 9a of [44]), suggesting that the free energy barriers responsible for hysteresis were lowered in the former case. Moreover, the curve of nearly reversible sorption/desorption at the higher temperature (Fig. 1(b)) passes roughly through the center of the hysteresis "window" between the first sorption and desorption curves (Fig. 1(a)) over a wide range of low humidities ($h < 60\%$). The data in Fig. 1(b) also makes the tantalizing suggestion of lingering hysteresis in the multilayer regime at an elevated temperature where hysteresis is already suppressed in the monolayer regime. This is consistent with our prediction that the critical temperature for condensation of larger droplets in nanopores is much larger than for individual adatoms in the first monolayer, as shown in Figure. 10.

- **Cycling History Dependence:** Although we do not claim a quantitative understanding, it makes perfect sense in light of our theory that the first few sorption/desorption cycles often exhibit strong history dependence, where hysteresis grows with time, until a more reproducible path is achieved. This would naturally result from trapped condensed phases (droplets or bubbles) in the adsorbate, which may require nucleation to a larger perturbation to be released, e.g. from defects, cracks, or chemical heterogeneities. As explained above in the context of nanopore junctions, any heterogeneity can act as a pinning site for the adsorbate, effectively removing mass and increasing internal resistance during the initial sorption and desorption cycles. Of course, the same behavior is observed in rechargeable batteries, where the first few cycles are often very different from next hundred, e.g. due to the lithium trapping in interfacial films or defect sites, which lead to an irreversible initial capacity loss.

Conclusion

We have developed a simple thermodynamic theory of sorption/desorption hysteresis in nano porous solids, based on the concept of hindered molecular condensation. The model makes a number of novel and testable predictions that seem consistent with previously unexplained data for cement paste and concrete, without postulating any pore collapse. Further experiments to systematically study the effects of temperature, humidity sweep rate, cycling behavior, etc., are proposed. The theory is very general and could be refined at the nanoscale and connected with macroscopic transport and mechanical deformation. The possibility of making quantitative predictions directly from the microstructure may lead to new, more accurate methods of determining the internal surface area and nanopore width distribution directly from the observed hysteresis of sorption and desorption isotherms. For concrete in particular, fruitful new directions for experiments suggested by our theory would involve systematically varying the temperature and humidity sweep rate during sorption/desorption of water vapor.

Acknowledgments: This research was funded by NSF Eager Collaborative Grants 1153509 to MIT and 1153494 to Northwestern University. The MIT Concrete Sustainability Hub also provided some support for this part (MZB). Preliminary work was also funded by NSF under Grant DMS-0948071 to MIT (MZB) and Grant CMS-0556323 to Northwestern University (ZPB) and by the U.S. DoT Grant 27323 provided through the Infrastructure Technology Institute of Northwestern University (ZPB). The authors thank Rolland J.-M. Pellenq for valuable comments and references.

References

[1] Bažant, Z. P. and Bazant, M. Z., "Theory of sorption hysteresis in nanoporous solids: I. Snap-through instabilities", submitted. Online preprint arXiv:1108.4949v1 [physics.flu-dyn].

[2] Adolphs, J., and Setzer, M.J. (1996). "A model to describe adsorption isotherms." *J. of Colloid and Interface Science* 180, 70–76.

[3] Adolphs, J., Setzer, M.J. and Heine, P. (2002). "Changes in pore structure and mercury contact angle of hardened cement paste depending on relative humidity." *Materials and Structures* 35, 477–486.

[4] Balbuena, P.B., Berry, D., and Gubbins, K.E. (1993). "Solvation pressures for simple fluids in micropores." *J. Phys. Chem.* 97, 937–943.

[5] Bažant, Z.P. (1970). "Constitutive equation for concrete creep and shrinkage based on thermodynamics of multi-phase systems." *Materials and Structures*, 3, 3–36 (reprinted in *Fifty Years of Evolution of Science and Technology of Building Materials and Structures*, Ed. by F.H. Wittmann, RILEM, Aedificatio Publishers, Freiburg, Germany 1997, 377–410).

[6] Bažant, Z.P. (1970). "Delayed thermal dilatations of cement paste and concrete due to mass transport." *Nuclear Engineering & Design*, 24, 308–318.

[7] Bažant, Z.P. (1972). "Thermodynamics of interacting continua with surfaces and creep analysis of concrete structures." *Nuclear Engineering and Design*, 20, 477–505.

[8] Bažant, Z.P. (1972). "Thermodynamics of hindered adsorption with application to cement paste and concrete." *Cement and Concrete Research*, 2, 1–16.

[9] Bažant, Z.P. (1975)."Theory of creep and shrinkage in concrete structures: A précis of recent developments", *Mechanics Today*, ed. by S. Nemat-Nasser (Am. Acad. Mech.), Pergamon Press 1975, Vol. 2, pp. 1–93.

[10] Bažant, Z.P., and Cedolin, L. (1991). *Stability of Structures: Elastic, Inelastic, Fracture and Damage Theories*, Oxford University Press, New York; 2nd. ed. Dover Publ. 2003; 3rd ed. World Scientific Publishing, Singapore–New Jersey–London 2010.

[11] Bažant, Z.P., and Moschovidis, Z. (1973). "Surface diffusion theory for the drying creep effect in Portland cement paste and concrete" *J. Am. Ceramic Soc.*, 56, 235–241.

[12] Bonnaud, P.A., Coasne, B., and Pellenq, R.J.-M. (2010). "Molecular simulation of water confined in nanoporous silica." *J. Phys.: Condens. Matter*, 284110 (15pp).

[13] Brochard, L., Vandamme, M. and Pellenq, R.J.-M. (2011). Competitive adsorption of carbon dioxide and methane in coal." Privately communicated manuscript; submitted to PNAS

[14] Brochard, L., Vandamme, M. and Pellenq, R.J.-M. (2011). Poromechanics of nanoporous media." Privately communicated manuscript; submitted to *J. of the Mech. and Phys. of Solids.*

[15] Brunauer, S. (1943). *The adsorption of gases and vapors.* Princeton University Press, Princeton, NJ, 1943 (p. 398).

[16] Cohan, L. H. (1938) "Sorption hysteresis and the vapor pressure of concave surfaces", *J. Am. Chem. Soc.* 60, 430-435.

[17] Brunauer, S., Emmett, P.T., and Teller, E. (1838). "Adsorption of gases in multi-molecular layers." *J. Amer. Chemical Soc.* 60, 309–319.

[18] Gelb, L. D., Gubbins, K. E., Radhakrishnan, R. and Sliwinska-Bartkowiak, M. (1999) ”Phase separation in confined systems”, Rep. Prog. Phys. 62, 1573-1659.

[19] Pellenq, R. J.-M. and Levitz, P. E. (2002) ”Capillary condensation in a disordered mesoporous medium: a grand canonical Monte Carlo study”, *Molecular Physics*, 100, 2059-2077.

[20] B. Coasne, A. Galarneua, F. Di Renzo, and R. J.-M. Pellenq (2007) ”Effect of morphological defects on gas adsorption in nano porous silicas” *J. Phys. Chem. C*, 111, 15759-15770.

[21] B. Coasne, A. Galarneau, F. Di Renzo, and R. J.-M. Pellenq (2009). “Intrusion and retraction of fluids in nanopores: effect of morphological heterogeneity”, *J. Phys. Chem. C* 113, 1953-1962.

[22] B. Coasne, A. Galarneau, F. Di Renzo, and R. J.-M. Pellenq (2008). “Molecular simulation of adsorption and intrusion in nanopores.” *Adsorption* (2008) 14: 215-221.

[23] B. Coasne, F. Di Renzo, A. Galarneau and R.J.-M. Pellenq (2008). “Adsorption of simple fluid on silica surface and nanopore: effect of surface chemistry and pore shape.” *Langmuir* 24, 7285–7293

[24] Derjaguin, B.V. (1940). “On the repulsive forces between charged colloid particles and the theory of slow caogulation and stability of lyophole sols, *Trans. of the Faraday Society* 36, 203, 730.

[25] Espinosa, R.M., and Franke, L. (2006). “Influence of the age and drying process on pore structure and sorption isotherms of hardened cement paste.” *Cement and Concrete Research* 36 (2006) 1969-1984 (Figs. 2, 6, 16).

[26] Feldman, R.F., and Sereda, P.J. (1964). “Sorption of water on compacts of bottle hydrated cement. I: The sorption and length-change isotherms.” *J. Appl. Chem.* 14, p.87.

[27] Feldman, R.F., and Sereda, P.J. (1968). “A model for hydrated Portland cement paste as deduced from sorption-length change and mechanical properties.” Materials and Structures 1 (6) (1968) 509–520.

[28] Frenkel, D., and Smit, B. (1996). *Understanding Molecular Simulations.* Academic Press, Sand Diego–New York.

[29] Jennings, H.M. (2000). “A model for the microstructure of calcium silicate hydrate in cement paste.” Cement and Concrete Research 30, 101–116.

[30] Jennings, H.M. (2010). “Pores and viscoelastic properties of cement paste.” submitted to an Elsevier Science journal.

[31] Jennings, H.M., Bullard, J.W., Thomas, J.J., Andrade, J.E., Chen, J.J., and Scherer, G.W. (2008). “Characterization and modeling of pores and surfaces in cement paste: Correlations to processing and properties.” *J. of the Advanced Concrete Technology* 6 (1), 5–29.

[32] Jönson, B., Nonat, A., Labbez, C., Cabane, B., and Wennerström, H. (2005). “Controlling the cohesion of cement paste.” *Langmuir* 21, 9211-9221.

[33] Jönson, B., Wennerström, H. Nonat, A., and Cabane, B. (2004). “Onset of cohesion in cement paste.” *Langmuir* 20, 6702–6709.

[34] Malani, A., Ayappa, K.G., and Murad, S. (2009). “Influence of hydrophillic surface specificity on the structural properties of confined water.” *J. Phys. Chem.* 113, 13825–13839.

[35] Pellenq, R. J.-M., Kushima, A., Shashavari, R., Van Vliet, K.J., Buehler, M.J., Yip, S. and Ulm, F.-J. (2010). “A realistic molecular model of cement hydrates.” *Proc. Nat. Academy of Sciences* 106 (38), 16102–17107.

[36] Powers, T.C., and T.L. Brownyard (1946), “Studies of the Physical Properties of Hardened Portland Cement Paste. Part 2. Studies of Water Fixation”. *J. of the Am. Concrete Institute* 18(3), 249–336.

[37] Powers, T.C. (1966). “Some observations on the interpretation of creep data.” *Bulletin RILEM (Paris)*, p. 381.

[38] Rarick, R.L., Bhatty, J.W. and Jennings, H.M. (1995). “Surface area measurement using gas sorption: Application to cement paste.” *Material Science of Concrete IV*, editied by J. Skalny and S. Mindess, Am. Ceramic Soc., Chapter 1, pp. 1–41.

[39] Scherer, G.W. (1999). “Structure and properties of gels.” *Cement and Concrete Research* 29 (1999), 1149–1157.

[40] Smith, D.E., Wang, Y., Chaturvedi, A., Whitley, H.D. (2006). "Molecular simulations of the pressure, temperature, and chemical potential dependencies of clay swelling." *J. Phys. Chem. B* 110, 20046–20054.

[41] Thomas, J.J., Allen, A.J., and Jennings, H.M. (2008). "Structural changes to the calcium hydrate gel phase of hydrated cement with age, drying and resaturation." *J. of the Am. Ceramic Soc.* 91 (10), 3362–3369.

[42] Bažant, Z.P., Asghari, A. A., and Schmidt, J. (1976). "Experimental study of creep of hardened cement paste at variable water content." *Materials and Structures* (RILEM, Paris),9, 279–190.

[43] Bažant, Z.P., and Raftshol, W. J. (1982). "Effect of cracking in drying and shrinkage specimens." *Cement and Concrete Research*, 12, 209–226; Disc. 797–798.

[44] Baroghel-Bouny, V. (2007) "Water vapour sorption experiments on hardened cementitious materials Part I: Essential tool for analysis of hygral behaviour and its relation to pore structure" *Cement and Concrete Research* 37, 414437.

[45] Romero-Vargas Castrillón, S., Giovambattista, N., Aksay, I. A., Debenedetti, P. G. (2011) "Structure and Energetics of Thin Film Water," *J. Phys. Chem. C* , 115, 46244635.

[46] Suresh, S.J., and Naik, V. M. (2000)."Hydrogen bond thermodynamic properties of water from dielectric constant data". *Journal of Chemical Physics*, 113, 9727?9732.

[47] Bažant, Z.P., and Najjar, L. J. (1972). "Nonlinear water diffusion in nonsaturated concrete." *Materials and Structures* (RILEM, Paris), 5, 3–20 (reprinted in *Fifty Years of Evolution of Science and Technology of Building Materials and Structures*, Ed. by F.H. Wittmann, RILEM, Aedificatio Publishers, Freiburg, Germany 1997, 435–456).

[48] Bažant, Z.P., and Kaplan, M.F. (1996). *Concrete at High Temperatures: Material Properties and Mathematical Models*, Longman (Addison-Wesley), London (monograph and reference volume, 412 + xii pp.) (2nd printing Pearson Education, Edinburgh, 2002).

[49] Cerofolini, G.F., Meda, L. (1998). "A theory of multilayer adsorption on rough surfaces in terms of clustering and melting BET piles." *Surface Science* 416, 402–432.

[50] Cerofolini, G.F., Meda, L. (1998). "Clustering and melting in multilayer equilibrium adsorption." *J. of Colloid and Interface Science* 202, 104–123.

[51] Nikitas, P. (1996). "A simple statistical mechanical approach for studying multilayer adsorption: Extensions of the BET adsorption isotherm." *J. Phys. Chem.* 100, 15247–15254.

[52] Seri-Levy, A. and Avnir, D. (1993) "The Brunauer-Emmett-Teller Equation and the effects of lateral interactions: A simulation study", *Langmuir* 9, 2523-2529.

[53] Liu, H., Zhang, L., and Seaton, N. A. (1993) "Analysis of sorption hysteresis in mesoporous solids using a pore network model", *Journal of Colloid and Interface Science* 156, 285-293.

[54] Hirth, J. P. and Lothe, J., *Theory of Dislocations*, (Kreiger, 1992).

[55] Guggenheim, E. A. *Mixtures* (Oxford University Press, London, 1952).

[56] Cahn, J. W. and Hilliard, J. E. (1958) "Free energy of a nonuniform system. I. Interfacial energy," *J. Chem. Phys.* 28, 258.

[57] Vandamme, M., Brochard, L., Lecampion, B. and Coussy, O. (2010) "Adsorption and strain: The CO2-induced swelling of coal," *J. of the Mechanics and Physics of Solids* 58, 1489-1505.

[58] Thornton, K., Ågren, J. and Voorhees, P. W. (2003). "Modelling the evolution of phase boundaries in solids at the meso- and nano-scales", *Acta Materialia* 51, 56755710.

[59] Baluffi, R., Allen, S. A. and Carter, W. C (2005) *Kinetics of Materials* (Wiley, New York, 2005).

[60] , Bazant, Martin Z. (2011) *10.626 Electrochemical Energy Systems* (Massachusetts Institute of Technology: MIT OpenCourseWare), http://ocw.mit.edu. License: Creative Commons BY-NC-SA.

[61] Meethong, N., Huang, H. Y. S., . Carter, W. C., and Chiang, Y. M. (2007) "Size-Dependent Lithium Miscibility Gap in Nanoscale $\mathrm{Li}_1 - x\mathrm{FePO}_4$", *Electrochemical and Solid-State Letters* 10, A134-A138.

[62] Meethong, N., Huang, H. Y. S., Speakman, S. A. Carter, W. C., and Chiang, Y. M. (2007) "Strain Accommodation during Phase Transformations in Olivine?Based Cathodes as a Materials Selection Criterion for High?Power Rechargeable Batteries", *Advanced Functional Materials* 17, 1115.

[63] Wagemaker, M., Singh, D. P., Borghols, W. J. H., Lafont, U., Haverkate, L., Peterson, V. K. and Mulder, F. M. (2011) "Dynamic Solubility Limits in Nanosized Olivine $\mathrm{LiFePO_4}$", *J. Am. Chem. Soc.*, 133, 1022210228.

[64] Harris, S. J., Timmons, A., Baker, D. R., and Monroe, C. (2010) "Direct *in situ* measurements of Li transport in Li-ion battery negative electrodes", *Chemical Physics Letters* 485, 265-274.

[65] Dreyer, W., Jamnik, J., Guhlke, C., Huth, R., Moškon, J., and Gaberšček, M. (2010). "The thermodynamic origin of hysteresis in insertion batteries." *Nature Materials* 9, 448–451.

[66] Dreyer, D., Guhlke, C., and Huth, R. (2011) "The behavior of a many-particle electrode in a lithium-ion battery", *Physica D* 240, 10081019

[67] Bai, P., Cogswell, D. A., and Bazant, M. Z. (2011) "Suppression of phase separation in $\mathrm{LiFePO_4}$ nanoparticles during battery discharge", preprint, arXiv:1108.2326v1 [cond-mat.mtrl-sci]

[68] Singh, G. K. , Ceder, G. and Bazant, M. Z. (2008) "Intercalation dynamics in rechargeable battery materials: General theory and phase transformation waves in $\mathrm{LiFePO_4}$," *Electrochimica Acta* 53, 7599.

[69] Burch, D. and Bazant, M. Z. (2009) "Size dependent spinodal and miscibility gaps in nanoparticles," *Nano Letters* 9, 3795.

[70] Cogswell, D. A. and Bazant, M. Z. (2011) "Coherency strain and the kinetics of phase separation in $\mathrm{LiFePO_4}$", preprint.

[71] Ferguson, T. R. and Bazant, M. Z., "Phase transformation dynamics in porous electrodes," in preparation. (Preliminary results were presented the Electrochemical Society Meetings in Montreal in May and in Boston in October, 2011.)

[72] Cahn, J. W. (1961) "On spinodal decomposition", *Acta Metallurgica*, 9, 795801.

[73] Padhi, A. K., Nanjundaswamy, K. S. and Goodenough, J. B. (1997) "Phospho-olivines as positive-electrode materials for rechargeable lithium batteries", *J. Electrochem. Soc.* 144, 1188-1194.

[74] Kang, B. and Ceder, G. (2009) "Battery materials for ultrafast charging and discharging", *Nature* 458, 190-193.

[75] Malik, R., Burch, D., Bazant, M. and Ceder, G. (2010) "Particle Size Dependence of the Ionic Diffusivity", *Nano Letters*10, 4123-4127.

[76] Malik, R., Zhou, F. and Ceder, G. (2011) "Kinetics of non-equilibrium lithium incorporation in $\mathrm{LiFePO_4}$", *Nature Materials*, 10 (8), 587-590.

[77] Pellenq, R. J.-M., Caillol, J. M., and Delville, A. (1997) "Electrostatic Attraction between Two Charged Surfaces: A (N,V,T) Monte Carlo Simulation", *J. Phys. Chem. B* 101, 8584-8594.

[78] Bazant, M. Z., Storey, B. D., and Kornyshev, A. A. (2011) "Double layer in ionic liquids: Overscreening versus crowding", *Physical Review Letters*, 106, 046102.

[79] Nauman, E. B. and Balsara, N. P. (1989) "Phase equilibria and the Landau-Ginzburg functional", *Fluid Phase Equilibria*, 45, 229-250.

[80] Nauman, E. B., Rousar, I. and Dutia, A. (1991) "On the ultimate fineness of a dispersion", *Chemical Engineering Communications*, 105, pp. 61-75.

[81] de Gennes, P. G. (1985) "Wetting: statics and dynamics", Rev. Mod. Phys. 57, 827-863.

[82] Israelachvili, J. *Intermolecular and Surface Forces* (Academic Press, New York, 1992).

[83] Rowlinson, J. S. and Widom, B. *Molecular Theory of Capillarity* (Clarendon Press, Oxford, 1984).

[84] Cahn, J. W. (1977) "Critical point wetting", J. Chem. Phys. 66, 3667 (1977).

[85] Gouin H. and Gavrilyuk, S. (2008) "Dynamics of liquid nanofilms", Int. J. Eng. Sci. 46, 1195-1202.

[86] Gouin H. (2009) "Liquid nanofilms: A mechanical model for the disjoining pressure ", Int. J. Eng. Sci. 47, 691-699.

[87] van der Waals, J. D. (1893). The thermodynamic theory of capillarity under the hypothesis of a continuous variation of density. (Translation by J. S. Rowlinson (1979)) Journal of Statistical Physics, 20, 197 (Original version: Zeitscherift fuer Physikalische Chemie, Stoechiometrie und Verwandtschaftslehre, 13, 657).

[88] Widom, B. (1999) "What do we know that van der Waals did not know?", Physica A, **263**, 500-515.

[89] Naumann, E. B. and He, D. Q. (2001) "Nonlinear diffusion and phase separation", *Chem. Eng. Science* 56, 1999-2018.